Slice of intraoceanic arc: Insights from the first multichannel seismic reflection profile across the South Sandwich island arc

Lieve E. Vanneste
Robert D. Larter
David K. Smythe*
British Antarctic Survey, High Cross, Madingley Road, Cambridge CB3 0ET, UK
Department of Geology and Applied Geology, University of Glasgow, Glasgow G12 8QQ, UK

ABSTRACT

We present the first multichannel seismic (MCS) reflection line that crosses the South Sandwich Trench, South Sandwich island arc, and East Scotia Sea backarc basin. The line is used in combination with earthquake catalogue data to interpret the strain distribution across the Sandwich plate and the relationship of forearc structures to processes operating at the trench. The MCS data reveal a 1.2-km-high fault scarp associated with a 20-km-wide arcward-tilted block in the mid-forearc; these features indicate large-scale gravitational collapse, and earthquake data are consistent with trench-normal extension at shallow depth in this area. There is, however, little evidence of distributed extension within the interior of the Sandwich plate. The MCS data show a small frontal wedge that achieves its maximum thickness only 18 km from the trench. Backarc magnetic data, mid-forearc extension, and the small size of the frontal wedge are all consistent with long-term and ongoing subduction erosion. Earthquake data suggest that this erosion is taking place in an environment of low interplate stress.

Keywords: earthquakes, South Sandwich Islands, seismic reflection data, subduction.

INTRODUCTION

Strain regimes in modern arc and forearc regions constitute a test for mechanical models that attempt to explain forces operating in subduction zones and the contribution of these forces to plate motions (Bird, 1978, 1998; Jarrard, 1986). Improved estimates of rates of sediment subduction and subduction erosion are needed in order to establish the global mass balance of continental crust and to assess their contribution to the evolution of the mantle (von Huene and Scholl, 1991). These two issues are linked by the fact that interplate stress is widely considered to influence the balance between accretion and subduction erosion, although opinions differ concerning the mechanism, and even the direction, of the effect (Cloos and Shreve, 1988; von Huene and Culotta, 1989; Vanneste and Larter, 2002).

Seismic profiling across modern arc-trench systems provides evidence relating to strain regime and the balance between accretion and erosion. The method is particularly effective when applied to intraoceanic subduction systems because these generally have a relatively short subduction history. This limits ambiguity concerning whether features are related to the present tectonic regime or are inherited.

The South Sandwich island arc is a classic intraoceanic arc in the southernmost Atlantic Ocean (Fig. 1). The South American plate converges with the Sandwich plate, on which the island arc is situated, at 70–85 mm/yr and is subducted at the South Sandwich Trench (Pelayo and Wiens, 1989). Farther west, the Sandwich plate is separating from the Scotia plate at the East Scotia Ridge, where the full spreading rate is 65–70 mm/yr (Livermore et al., 1997). This relatively simple tectonic setting has changed little since 15 Ma, except that the absolute and relative rates of motion of the Sandwich plate have accelerated since 7 Ma (Barker, 1995). Magnetic anomalies in the East Scotia Sea indicate that most of the present arc is on crust formed ca. 10 Ma (chron 5) at the East Scotia Ridge (Fig. 1). Therefore crust conjugate to that formed on the western flank of the ridge between 15 and 10 Ma (chrons 5B–5) must be beneath the modern inner forearc.

Here we present the first multichannel seis-

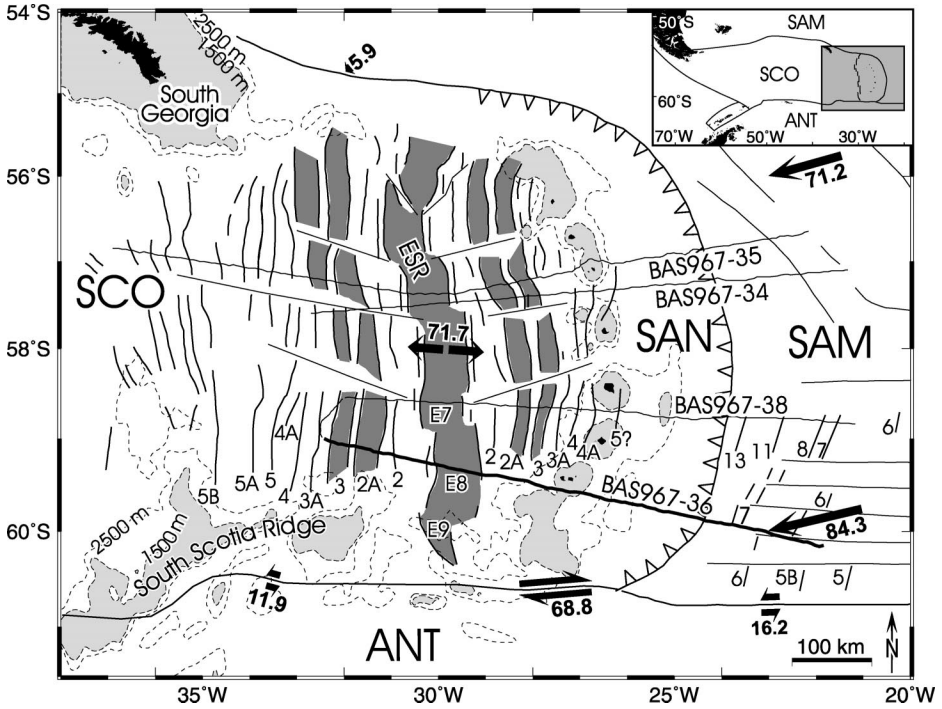

Figure 1. Magnetic anomaly map of East Scotia Sea, modified from Vanneste and Larter (2002). Gray box in inset shows location of map. Central Brunhes anomaly, as well as anomalies 2A and 3, are shaded dark gray. East Scotia Ridge (ESR) crest segments E7–E9 are labeled. Magnetic-anomaly identifications on South American oceanic crust are based on Barker and Lawver (1988). Arrows indicate azimuths of relative motion between Scotia (SCO), Sandwich (SAN), South American (SAM), and Antarctic (ANT) plates, based on Euler vectors of Pelayo and Wiens (1989). Arrow lengths are proportional to rates (mm/yr). Locations of four Sandwich Lithospheric and Crustal Experiment (SLICE) multichannel seismic lines that cross trench, arc, and East Scotia Ridge are shown. Line BAS967-36, shown in Figures 2 (loose insert) and 3, is represented by thicker line; 2500 m contour (dashed line) and 1500 m contour (filled, light gray) define South Sandwich arc, South Georgia microcontinental block, and South Scotia Ridge. Barbed line represents trench.

*Present address: GeoLogica Ltd, 191 Wilton Street, Glasgow G20 6DF, UK.

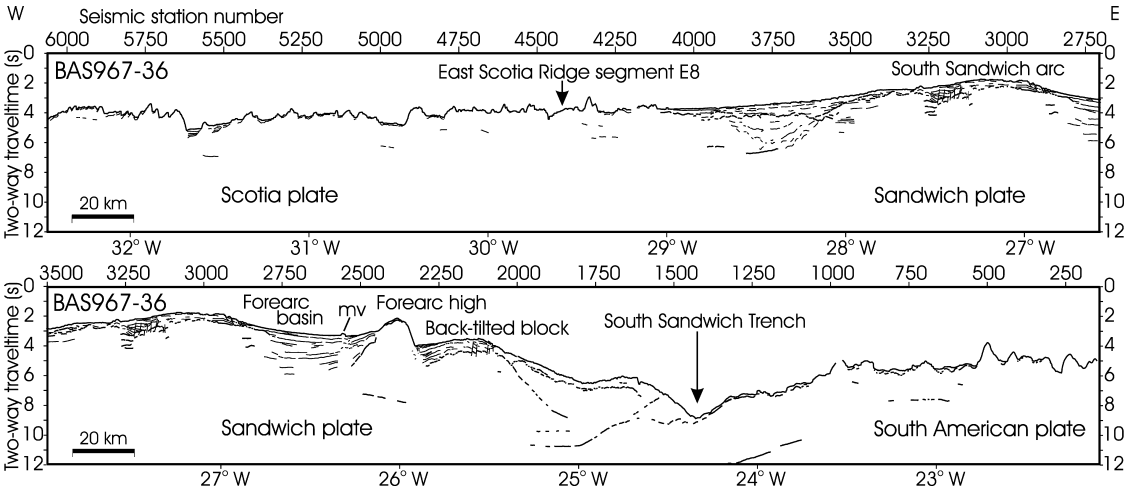

Figure 3. Interpreted line drawing of line BAS967-36 showing reflections identified on both migrated stack (Fig. 2, loose insert) and unmigrated stack; mv is mud volcano. Vertical exaggeration at seafloor is 6:1.

mic (MCS) line across the South Sandwich subduction system, together with earthquake data from a corridor parallel to the line. These data provide insights into the structure and evolution of this arc and the backarc basin. In particular, they show evidence of gravitational collapse of the outer forearc and only a small frontal wedge near the trench, suggesting that sediment subduction and subduction erosion have been important processes in the evolution of the South Sandwich arc.

SEISMIC REFLECTION DATA

The 600-km-long MCS line BAS967-36 was acquired during RRS *James Clark Ross* cruise JR18 as part of the Sandwich Lithospheric and Crustal Experiment (SLICE) (Larter et al., 1998). The line crosses the entire subduction system, from the outer rise in the east to the western flank of the backarc basin. An *f-k* migrated stack of the line is shown in Figure 2[1] and Figure 3 is an interpreted line drawing. The eastern end of the line shows a thin and irregularly distributed sediment cover (<200 m) over the crest of the outer rise, where the average seafloor depth is 3900 m. From ~50 km east of the trench, the outer rise exhibits a gentle westward dip down to the trench axis at a depth of 6680 m. The crest of the arc is 160 km west of the trench, measured along the line, and is ~1320 m deep. The line crosses East Scotia Ridge segment E8 ~140 km west of the arc crest.

Where the line crosses the trench, marine magnetic data (Barker and Lawver, 1988) indicate that the ocean crust currently being subducted has an age of 27 Ma (chron 8r). The trench sediments include at most 100 m of trench-fill sediment overlying ~200 m of ocean-basin sediment. A strong and fairly continuous reflection can be traced for nearly 50 km from the trench beneath the outer forearc until it is obscured by residual seafloor-multiple energy. We interpret this reflection as the top of subducted oceanic basement.

The outer forearc slope has a stepped appearance where the general trenchward dip is interrupted by two broad, gently arcward-dipping terraces. On the outer forearc slope, a 200–700-m-thick slope sediment apron with a chaotic seismic facies overlies a band of strong reflections. This band of reflections ends abruptly at station number (SN) 1610, 18 km west of the trench. East of this point the inner trench slope (SN 1430–1610) has an irregular surface and is the steepest part of the outer forearc slope, with an average dip of 6.6°. Beneath the inner trench slope is a frontal wedge with a thickness of as much as 2.5 s two-way traveltime (s TWTT) (>2.5 km) that has a seismic facies similar to that of the slope sediment apron, but distinct from the almost reflection-free material beneath the slope apron to the west. The frontal wedge appears to taper arcward beneath the material to its west.

The forearc high, 90–100 km west of the trench, separates the outer forearc slope from a forearc basin covering the inner forearc. The top of the forearc high on this line, at 1590 m, is only slightly deeper than the crest of the arc. To the east, a 1200-m-high escarpment exposes reflection-free forearc basement and stands above a 20-km-wide arcward-dipping terrace. Stratified sediments to 1.3 s TWTT thick (>1 km) are beneath the terrace. Within these sediments there is a change in reflection geometry, from parallel with the top of basement to flat lying in the near surface closest to the escarpment. Small normal faults that offset the seafloor are present at the trenchward edge of the terrace. East of the terrace, breaks in slope of the seafloor (at SN 2040) and of the base of the slope sediment apron (at SN 2020) coincide with the upward projection of a 20-km-long, trenchward-dipping, weak and discontinuous reflection, which we interpret as a low-angle detachment fault.

The inner forearc basin reaches a thickness of >3 s TWTT (>4 km). Reflections on the eastern flank of the basin show arcward divergence and onlap the forearc high. The data do not show a distinct western boundary to the forearc basin; instead, reflections become less continuous and eventually merge into the chaotic facies beneath the arc. The seafloor over the basin is concave upward, except for a 100-m-high mound in the deepest part, that is situated over a fault. We interpret this mound as a mud volcano formed by escape of fluids from rapidly deposited forearc-basin sediments.

West of the arc crest, a sedimentary apron to 1.0 s TWTT thick (<1 km) covers most of the backarc basement east of the East Scotia Ridge. In contrast, the sediment cover on the western flank of the backarc basin is as much as 500 m thick in places, but absent elsewhere. The seafloor on the steepest part of the slope west of the arc (SN 3400–3700) has a stepped appearance with small westward-facing scarps separated by gently arcward-dipping terraces. We interpret this geometry as evidence of gravitational instability within the sedimentary apron.

Along most of its 90 km length, ridge segment E8 exhibits a median valley ~12 km wide with 300–800 m relief (Bruguier and Livermore, 2001). However, a topographic high, offset toward the eastern wall, occurs within the valley where line BAS967-36 crosses it (SN 4350–4480). Most abyssal hills west of the East Scotia Ridge have steep ridgeward flanks and gentler western flanks, suggesting that the spreading process involved rotational block faulting.

The oceanic basement of both the South

[1]Loose insert: Figure 2. Migrated stack of line BAS967-36.

American plate and the backarc basin west of SN 3870 appear mostly reflection free. In contrast, rich basement reflectivity has been observed in both the North Atlantic and Pacific, which formed at slow and fast spreading rates, respectively. Such reflectivity is thought to result from structural and/or magmatic processes close to spreading centers (Ranero et al., 1997; Reston et al., 1999). We interpret the scarcity of reflections within oceanic basement on line BAS967-36 as a consequence of scattering of seismic energy at the irregular and thinly sediment-covered top of oceanic basement. The only area of rich reflectivity in the backarc basement is 50–80 km west of the arc crest (SN 3570–3870), where the slope sediment apron is thickest. The most prominent reflections dip westward, but there are others that dip eastward. Some extend to 2 s TWTT beneath the top of basement and therefore probably to the backarc Moho. The upward projection of the easternmost of these reflections coincides with the location where the overall dip of the top of basement changes from westward, down from the arc, to gently eastward, away from the East Scotia Ridge.

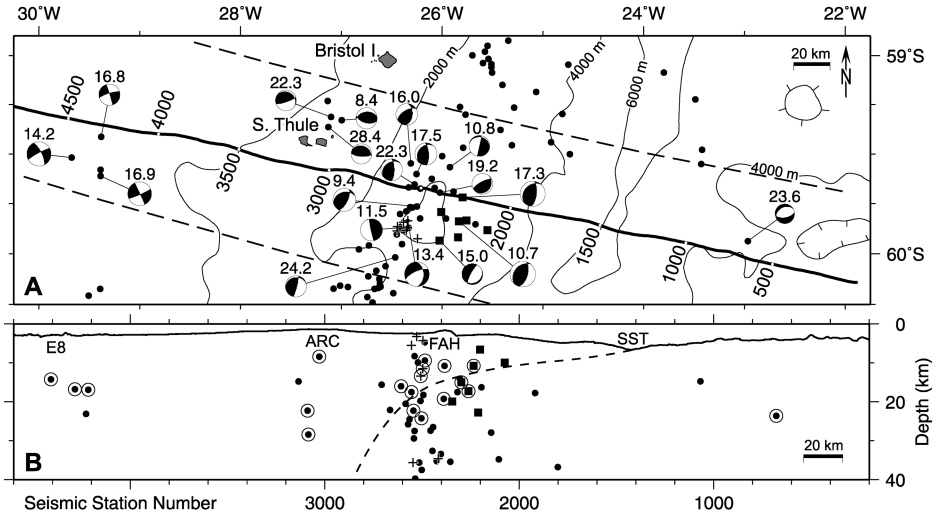

Figure 4. A: Map showing all earthquake hypocenters from catalogue of Engdahl et al. (1998) for earthquakes that occurred near line BAS967-36 (heavy line) from 1964 to 1998, were <40 km deep, were recorded by at least 20 stations, and for which at least one depth phase has been identified. Earthquakes marked by filled squares were part of swarm that occurred on 9–10 March 1993, and those marked by crosses were part of swarm on 5 April 1993. All other earthquakes are shown as dots. Dashed lines indicate limits of 100-km-wide corridor used as basis for section in B. Where available, focal mechanisms from Harvard Centroid Moment Tensor (CMT) catalogue are shown for events inside this corridor at <30 km depth. Numbers above each CMT are hypocentral depths in kilometers from Engdahl et al. (1998) catalogue. Seismic station numbers along line BAS967-36 are annotated and marked by white dots. Bathymetric contours are shown at 2000 m intervals, based on global seafloor-topography data of Smith and Sandwell (1997). B: Cross section along line BAS967-36 showing hypocenters of earthquakes within corridor marked by dashed lines in A, projected onto line along azimuth 20°/200°. Earthquakes for which CMT focal mechanisms are shown in A are circled. Other symbols as in A. Solid line represents bathymetric profile obtained from line BAS967-36 (assumed water velocity of 1500 m/s). Dashed line represents inferred top of subducted slab. Ridge-crest segment E8 is labeled, as well as forearc high (FAH) and South Sandwich Trench (SST).

EARTHQUAKE DATA

Locations and focal mechanisms of shallow earthquakes provide a complementary source of information on strain distribution across the Sandwich plate. Locations of earthquakes from the catalogue of Engdahl et al. (1998) that satisfy certain quality criteria are shown in Figure 4A. The hypocenters of those earthquakes that are within a 100-km-wide corridor centered on the MCS line were projected onto the line and are shown in cross section in Figure 4B.

The Harvard Centroid Moment Tensor (CMT) catalogue includes focal mechanisms indicating strike-slip faulting for three earthquakes near East Scotia Ridge segment E8. These events probably occurred in the overlap zone between segments E8 and E9 (Wetzel et al., 1993; Bruguier and Livermore, 2001). Engdahl et al. (1998) located one of these earthquakes in the overlap zone and the other two ~10 km east of it. That these calculated locations are so close to where we infer the events occurred, and the location of another small cluster of earthquakes beneath the arc, enhances our confidence in the accuracy of the forearc hypocenter locations.

Figure 4 shows that shallow seismicity is concentrated in the mid-forearc and that there is relatively little activity within 40 km of the arc. Two earthquake swarms that occurred in 1993 account for 14 hypocenters, but even if these are disregarded there remains a significant concentration of seismicity in the mid-forearc. Above 15 km, the arcward limit of the more seismically active part of the forearc coincides with the mud volcano on the MCS line.

CMT focal mechanisms exist for 12 of the mid-forearc earthquakes shallower than 30 km in Figure 4. Engdahl et al. (1998) identified two or more depth phases for each of these events and calculated a standard error in depth of <6 km for all but two of them. Allowing for the uncertainties in depths, the focal mechanisms and hypocentral depths of these events suggest a change in the style of faulting at <19 km depth. One earthquake beneath the forearc high with a calculated hypocentral depth of 13.4 km has a focal mechanism that clearly indicates southeast-northwest extension, and three others with depths of <16 km can be interpreted as steep normal faulting associated with east-west to southeast-northwest extension. However, eight forearc earthquakes have focal mechanisms indicating east-west to southeast-northwest shortening, and the shallowest of these has a depth of 9.4 km (±9.1 km at 2σ). These observations suggest that either the boundary between the forearc and the subducting slab is at relatively shallow depth beneath the forearc high, with low-angle subduction beneath the outer forearc, or extensional faulting in the mid-forearc occurs above an intraforearc detachment at <19 km depth. The zone of concentrated seismicity beneath the mid-forearc actually extends to >100 km depth, which suggests that this is where most slab bending occurs, and is consistent with low-angle subduction beneath the outer forearc.

The magnitudes of the largest forearc earthquakes are low compared to most other subduction zones. Only four of the forearc events shown in Figure 4 have moment magnitudes of >6.0, the largest being 6.9.

DISCUSSION AND CONCLUSIONS

MCS line BAS967-36 and coincident earthquake data reveal evidence of trench-normal extensional faulting in the mid-forearc, but there is no evidence of extensional faulting affecting the arc. The lack of extension in the arc is surprising, because Jarrard's (1986) statistical analysis predicts that the most extensional strain regime among all modern arcs should occur here. By stepwise multiple regression, Jarrard (1986) found that extension in modern arcs is favored by a combination of slow convergence rate (relative to the major overriding plate, i.e., the Scotia plate in this case), high slab age, and high slab dip to 100 km depth. Our observations suggest that tectonic strain in the South Sandwich subduction

system is accommodated mainly by backarc spreading, rather than by distributed extension throughout the Sandwich plate. The lack of evidence for distributed extension suggests to us that the most likely cause of the mid-forearc extension is gravitational instability resulting from subduction erosion, rather than regional tectonic stress.

Based on sidescan sonar and four-channel seismic reflection data, Vanneste and Larter (2002) interpreted a trench-normal extensional strain regime in the northern South Sandwich outer forearc. The mid-forearc in that area includes a 1500-m-high scarp above an arcward-tilted terrace to the east. The MCS data presented here show that a similar arcward-tilted terrace in the southern forearc is the top of a rotated fault block, and the form of the adjacent forearc high is consistent with the suggestion by Vanneste and Larter (2002) that such highs are produced by flexural footwall uplift. For a semiinfinite elastic plate subjected to a line load at its end and no external torque, Turcotte and Schubert (1982) showed that a point of zero deflection is reached at a distance $x = (\pi/2)\alpha$, where α is the flexural parameter

$$\alpha = \left[\frac{4D}{(\rho_m - \rho_s)g}\right]^{1/4} \quad (1)$$

that depends on the rigidity D and the buoyancy (ρ) difference between the mantle and the sediments overlying the plate. Here, the shape of the deepest forearc basin reflections suggests that a point of zero deflection is reached 40–50 km arcward of the fault, implying that α is 25–32 km. If a density difference of 1300 kg m^{-3} between mantle and sediments is assumed, equation 1 indicates that D is in the range 1.3–3.4 $\times$ 10^{21} Nm. For a plate with a Young's modulus of 70 GPa and a Poisson's ratio of 0.25, this range of D is equivalent to an elastic thickness in the range 6–8 km. This thickness is within the range predicted by Watts et al. (1980) for 10 Ma oceanic lithosphere, and 10 Ma is our estimate of the average age of the lithosphere beneath this part of the forearc basin (see following).

The width of the rotated fault block, and earthquake focal mechanisms in the mid-forearc, suggest that extensional strain extends to many kilometers depth, and probably to the décollement. The observation that the arcward limit of forearc seismicity at depths <15 km approximately coincides with the fault beneath the mud volcano suggests that this is now the master fault bounding the deforming part of the forearc.

The MCS line shows that a frontal wedge achieves its maximum thickness 18 km from the trench and then tapers arcward. Even though the sediment cover on the outer rise is thin and discontinuous, if it was all accreted it would form a frontal wedge of this size in ~5 m.y. Therefore most of the sediment entering the trench since the start of East Scotia Sea opening (before 15 Ma) must have been subducted. On the basis of previous work on the northern part of the forearc (Vanneste and Larter, 2002), we consider it likely that the frontal wedge is composed largely of trench sediments derived from the forearc slope, and that little or no ocean-floor sediment has been accreted. Trenchward thickening of the slope sediment apron is the opposite of what would be expected for the sediment cover overlying a growing accretionary prism.

Backarc magnetic data indicate that most of the present arc is on crust formed ca. 10 Ma at the East Scotia Ridge (Fig. 1) and that the basement of the modern inner forearc originated as backarc crust. The southernmost part of the arc appears to be on backarc crust that is younger than 8 Ma (chron 4), and if spreading was symmetric during the early stages of backarc opening, even the basement beneath the forearc high formed since 12.5 Ma (Fig. 1). These crustal ages imply that either backarc spreading in this area was initiated within 60 km of the trench or extensive subduction erosion has taken place. The small frontal wedge and the evidence of trench-normal extension in the mid-forearc are consistent with long-term and ongoing subduction erosion. The relatively low magnitude of the largest forearc earthquakes indicates that this subduction erosion is taking place in an environment of low interplate stress.

ACKNOWLEDGMENTS

We thank everyone who participated in RRS *James Clark Ross* cruise JR18. We are especially grateful to David Abensour, whose innovative adaptation of old seismic recording equipment spared us from the ordeal of working with hundreds of 9-track tapes.

REFERENCES CITED

Barker, P.F., 1995, Tectonic framework of the East Scotia Sea, *in* Taylor, B., ed., Backarc basins: Tectonics and magmatism: New York, Plenum Press, p. 281–314.

Barker, P.F., and Lawver, L.A., 1988, South American–Antarctic plate motion over the past 50 Myr, and the evolution of the South American–Antarctic Ridge: Royal Astronomical Society Geophysical Journal, v. 94, p. 377–386.

Bird, P., 1978, Stress and temperature in subduction shear zones: Tonga and Mariana: Royal Astronomical Society Geophysical Journal, v. 55, p. 411–434.

Bird, P., 1998, Testing hypotheses on plate-driving mechanisms with global lithosphere models including topography, thermal structure and faults: Journal of Geophysical Research, v. 103, p. 10 115–10 129.

Bruguier, N.J., and Livermore, R.A., 2001, Enhanced magma supply at the southern East Scotia Ridge: Evidence for mantle flow around the subducting slab?: Earth and Planetary Science Letters, v. 191, p. 129–144.

Cloos, M., and Shreve, R.L., 1988, Subduction-channel model of prism accretion, melange formation, sediment subduction, and subduction erosion at convergent plate margins: 1. Background and description: Pure and Applied Geophysics, v. 128, p. 455–500.

Engdahl, R.E., Van der Hilst, R., and Bulland, R., 1998, Teleseismic earthquake relocation with improved travel times and procedures for depth determination: Seismological Society of America Bulletin, v. 88, p. 722–743.

Jarrard, R.D., 1986, Relations among subduction parameters: Reviews of Geophysics, v. 24, p. 217–284.

Larter, R.D., King, E.C., Leat, P.T., Reading, A.M., Smellie, J.L., and Smythe, D.K., 1998, South Sandwich slices reveal much about arc structure, geodynamics and composition: Eos (Transactions, American Geophysical Union), v. 79, p. 281, 284–285.

Livermore, R., Cunningham, A., Vanneste, L., and Larter, R., 1997, Subduction influence on magma supply at the East Scotia Ridge: Earth and Planetary Science Letters, v. 150, p. 261–275.

Pelayo, A.M., and Wiens, D.A., 1989, Seismotectonics and relative plate motion in the Scotia Sea region: Journal of Geophysical Research, v. 94, p. 7293–7320.

Ranero, C.R., Reston, T.J., Belykh, I., and Gnibidenko, H., 1997, Reflective oceanic crust formed at a fast-spreading center in the Pacific: Geology, v. 25, p. 499–502.

Reston, T.J., Ranero, C.R., and Belykh, I., 1999, The structure of Cretaceous oceanic crust of the NW Pacific: Constraints on processes at fast spreading centers: Journal of Geophysical Research, v. 104, p. 629–644.

Smith, W.H.F., and Sandwell, D.T., 1997, Global sea floor topography from satellite altimetry and ship depth soundings: Science, v. 277, p. 1956–1962.

Turcotte, D.L., and Schubert, G., 1982, Geodynamics, application of continuum physics to geological problems: New York, John Wiley and Sons, 450 p.

Vanneste, L.E., and Larter, R.D., 2002, Sediment subduction, subduction erosion and strain regime in the northern South Sandwich forearc: Journal of Geophysical Research (in press).

von Huene, R., and Culotta, R., 1989, Tectonic erosion at the front of the Japan Trench convergent margin: Tectonophysics, v. 160, p. 75–90.

von Huene, R., and Scholl, D.W., 1991, Observations at convergent margins concerning sediment subduction, subduction erosion, and the growth of continental crust: Reviews of Geophysics, v. 29, p. 279–316.

Watts, A.B., Bodine, J.H., and Ribe, N.M., 1980, Observations of flexure and the geological evolution of the Pacific Ocean basin: Nature, v. 283, p. 532–537.

Wetzel, L.R., Wiens, D.A., and Kleinrock, M.C., 1993, Evidence from earthquakes for bookshelf faulting at large non-transform ridge offsets: Nature, v. 362, p. 235–237.

Manuscript received January 31, 2002
Revised manuscript received May 17, 2002
Manuscript accepted May 21, 2002

Printed in USA

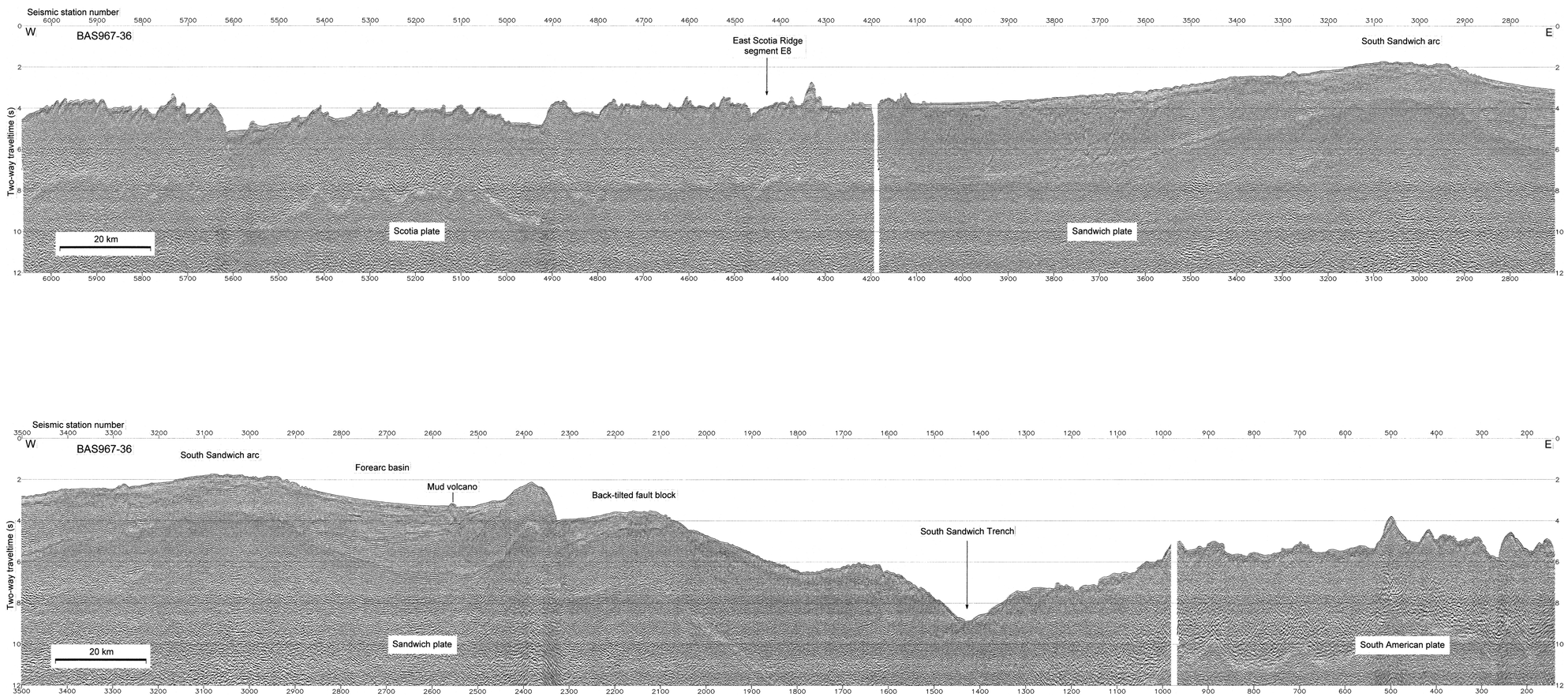

Figure 2. Migrated stack of line BAS967-36 (located in Fig. 1). Data acquired using array of 14 airguns with total volume of 98 L and nominal shot spacing of 100 m. Data recorded at 2 ms sampling interval from 96-channel, 2400-m-long streamer. Processing sequence included resampling to 4 ms, bandpass filtering, weighted-trace mix on shot gathers to attenuate coherent noise (station number [SN] 1–1250 and 4175–6066), predictive deconvolution, velocity analysis, *f-k* filter and inner-trace mute on CDP (common-depth point) gathers to suppress seafloor-multiple reflections (SN 2018–4175), 24-fold stack (25 m CDP bins), Stolt *f-k* migration, time-variable bandpass filter, weighted-trace mix, automatic gain control, and display bias. Vertical exaggeration at seafloor is 6:1.

Slice of intraoceanic arc: Insights from the first multichannel seismic reflection profile across the South Sandwich island arc
Lieve E. Vanneste, Robert D. Larter, David K. Smythe
Figure 2
Supplement to Geology, v. 30, no. 9
(September 2002)